Compact NEXAFS System Based on Laser–Plasma Soft X-ray Light Source for the Analysis of Barium Edges in a B+BaF$_2$ Optical Filter

T. Fok*, P. Wachulak, M. Wardzińska, A. Bartnik,
P. Nyga, M.P. Nowak and H. Fiedorowicz

Institute of Optoelectronics, Military University of Technology, S. Kaliskiego 2, 00-908 Warsaw 49, Poland

*e-mail: tomasz.fok@wat.edu.pl

In this work, we present the results of the analysis performed with near edge absorption fine structure spectroscopy of barium edges in a B+BaF$_2$ optical filter. The radiation was generated by a laser–plasma soft X-ray source based on a double-stream gas puff target. The use of a flat-field spectrometer based on a diffraction grating allowed us to collect the absorption spectra of the radiation transmitted by the analyzed optical filter. The results demonstrate the appearance of clear M-edges of barium (M4 and M5).

topics: near edge X-ray absorption fine structure (NEXAFS), soft X-rays, spectroscopy, barium

1. Introduction

The NEXAFS (near edge X-ray absorption fine structure) method was introduced more than 40 years ago by J. Stöhr [1] for the study of low-Z molecules absorbed by surfaces. Since then, this method has been widely used in many fields of science, for example in surface analysis in nanoscale samples [2, 3], thin organic films and liquids [4], and crystalline and amorphous inorganic materials [5].

Due to the high applicability of this measurement technique in the scientific world and the fact that it is mainly available on synchrotrons, a variety of compact solutions have been developed in the last few years, with a smaller number and range of photon energies [6–9] but still with a high and proven measurement potential.

In this paper, we present one of the potential applications of compact NEXAFS, i.e., the ability to detect barium (Ba) absorption edges (M-edges) using broadband plasma radiation from xenon and krypton. The analyzed material was a boron + barium fluoride (B+BaF$_2$) filter. The elements made of BaF$_2$ are widely used, for example, as optical windows, prisms, and lenses transmitting from ultraviolet to infrared [10], as scintillators to convert gamma radiation into detectable light [11, 12], to determine radiation quality in biology [13], and in microwave devices, especially at cryogenic temperatures due to its small losses at microwave frequencies [14]. Boron was used because it has a transmission window near ~ 6.6 nm, which was essential due to the filter's designated application. In this paper, barium M-edges are detected using a compact NEXAFS system.

2. Experimental setup

The measurements were performed on a setup previously presented in [15]. A significant modification was the change of the electromagnets, which resulted in different valve opening characteristics than in previous papers. As a result of this upgrade, the optimum gas pressures were reduced. The system shown in Fig. 1a had three sections: source section, sample section, and soft X-ray (SXR) spectrometer. The source section consisted of a laser–plasma source generating soft X-ray radiation (LPXS). The LPXS was driven by an Nd:YAG laser (model NL 303 HT, EKSPLA, Lithuania) with an energy of 0.6 J, pulse duration time of 3 ns, and a repetition rate of 10 Hz. The radiation was focused by a lens (diameter of 12.7 mm, a focal length f = 25 mm) to a spot of ~ 100 μm in diameter. A plasma was generated by the interaction of focused laser radiation with a double-stream Xe/He or Kr/He gas puff target [16, 17], which was formed by a collinear set of two nozzles driven by two electromagnetic valves. The inner nozzle is 0.8 mm in diameter and was pressurized by a high-Z gas, i.e., xenon and
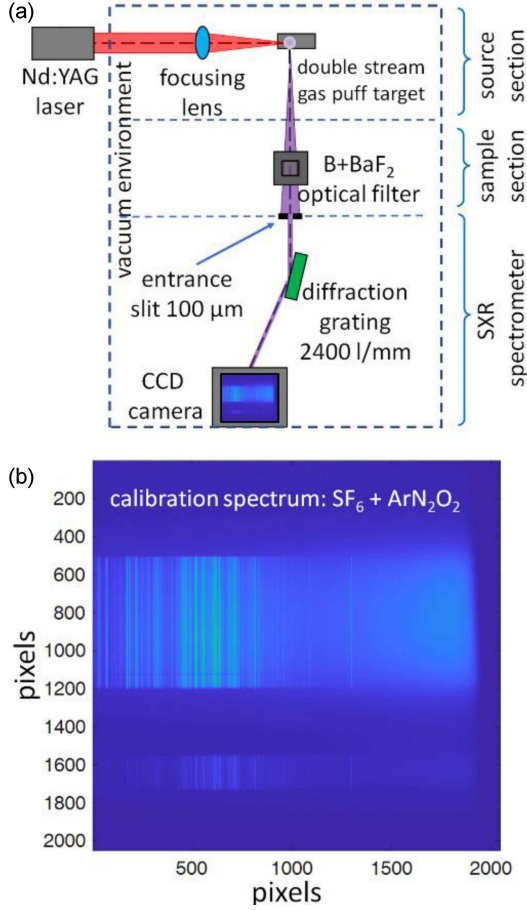
Fig. 1. (a) The NEXAFS experimental setup on which the spectrum of the radiation transmitted by the B+BaF$_2$ optical filter was measured and (b) the spectrum registered by the CDD camera — at the top is the reference spectrum, at the bottom is the sample spectrum.

krypton, to the optimal pressure of 8 bars, depending on the performed measurement. The outer nozzle was pressurized by a low-Z gas, i.e., helium, to 6.5 bars.

Further, the radiation was directed to the sample section, and after the interaction with the sample, part of the radiation was directed to the SXR spectrometer. The other part is later used as the reference signal. The SXR spectrometer with a similar configuration to the one described in [18] was used to produce and collect an absorption spectrum. The configuration was based on an entrance slit of 100 μm, a grazing incidence diffraction grating with a spatial frequency of 2400 l/mm (Hitachi), and a back-illuminated charge-coupled device (CCD) camera (GE 2048 2048 BI, greateyes, Germany). The camera had a chip with 2048×2048 pixels, with a pixel size of 13.5×13.5 μm^2. During the measurements, the chip was cooled to -20°C. A spectrometer with a comparable arrangement and a resolving power of $E/\Delta E = \sim 940$ was developed at the Institute of Optoelectronics [19].

The sample that was measured is an optical filter made of a 200 nm thick layer of boron and a 200 nm thick layer of barium fluoride deposited on top of the Si$_3$N$_4$ membrane with a thickness of 30 nm. Thin layers of barium fluoride and boron were deposited using an EB-PVD process (electron beam physical vapor deposition). This filter will be later used as a part of a source for photolithographic metrology near $\sim$ 6.7 nm wavelength.

Before obtaining the optical density spectra, a proper spectrometer calibration was necessary. The calibration spectra captured for Ar:N$_2$:O$_2$ gas mixture and SF$_6$ injected into the laser–target interaction region, depicted in Fig. 1b, allowed us to perform the procedure of SXR spectrometer calibration by constructing the calibration curve to match the camera's pixels with the photon energy [20]. To construct the calibration curve, we used positions of the fluorine line $\lambda = 1.6807$ nm from F^{8+} ion, oxygen line $\lambda = 2.1602$ nm from O^{6+} ion, two very intensive SXR nitrogen lines $\lambda = 2.489$ nm and $\lambda = 2.878$ nm from N^{5+} ions, and argon lines $\lambda = 4.873$ nm and $\lambda = 4.918$ nm from Ar^{8+} ions.

3. Results

During the measurements, two series of data were acquired: the first series for gas puff target made of xenon and helium, and the second series using krypton and helium gas puff target. To verify whether the lines detected by the spectrometer were from the measured filter, two additional data series were performed using the Si$_3$N$_4$ membrane alone without deposited layers.

For each series of data consisting of 16 CCD images, the background signal was measured, and calibration spectra were captured. During the data post-processing, the background signal was subtracted from each image. In every series of data, values from 16 images were integrated in order to increase the signal-to-noise ratio (SNR). Further, data from 150 CCD lines were integrated both in the reference spectrum and sample spectrum, which can be seen in Fig. 2a for Xe and Fig. 2b for Kr gas, which additionally increased SNR. The final optical density spectrum OD(E) is computed with the use of

$$\mathrm{OD}(E) = -\ln\left[\frac{S_{\mathrm{sam}}(E)}{S_{\mathrm{ref}}(E)}\right], \qquad (1)$$

where $S_{\mathrm{sam}}(E)$ and $S_{\mathrm{ref}}(E)$ are sample spectra and reference spectra, respectively. For a better visualization of the absorption edges, the obtained optical density spectrum is smoothed with a Golay–Savitzky (GS) filter (window = 3, frame length = 11) [21].

The spectra presented in Fig. 3a demonstrate two, M4 and M5, edges from barium obtained from measurement with Xe/He gas target. The edges look like peaks, due to the non-flat nature of the optical broad-band spectrum and the quite weak
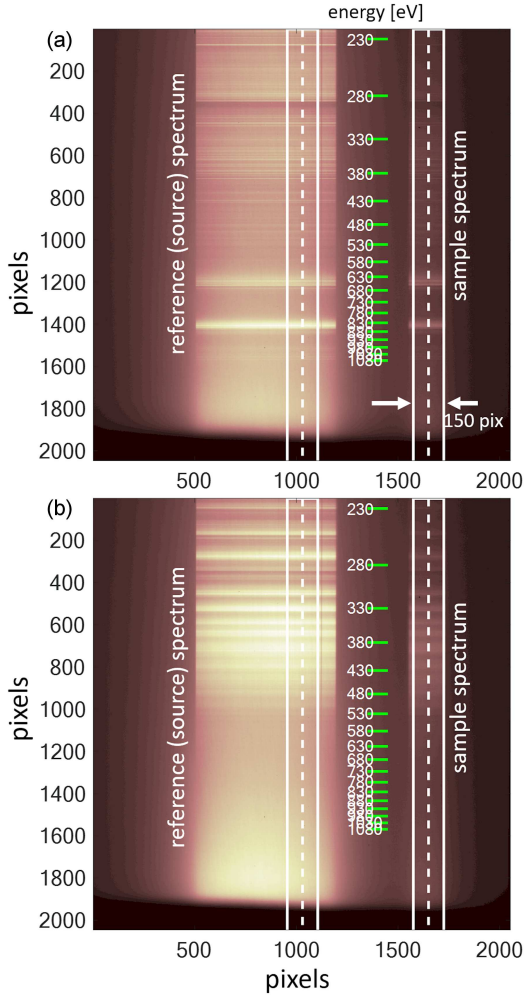
Fig. 2. Visualization of processing of images from the CCD camera taken for (a) xenon and (b) krypton as a working gas. Data from 150 CCD lines was integrated both for the reference and measured signals.

signal (the difference in OD signal of only 0.15 peak to valley). The M5 absorption edge occurs theoretically [22] at 780.5 eV, while the M4 edge can be found at 795.7 eV, while the measurements indicate slight energy offset, namely the M5 edge at 780.4 eV and M4 at 796.3 eV. The same edges are also visible for measurements performed with the Kr/He target (Fig. 3b), with a slight change in M5 edge energy equal to 780.5 eV — exactly as the database [22] predicts. The described values are compatible with the data from the Hephaestus database [22]. A group from Japan used mass spectrometry and X-ray absorption spectroscopy to study absorption edges in barium–oxide clusters. In their paper, they report M-edges from barium [23]. The other group confirmed the appearance of barium M-edges in $Ba_2Ca(BO_3)_2$ using X-ray excited optical luminescence (XEOL) spectroscopy [24]. These edges were also presented by a group from Switzerland [25]. They used X-ray
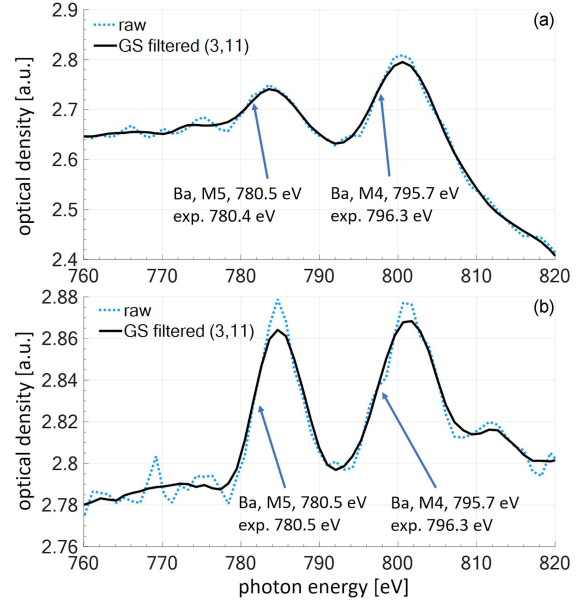
Fig. 3. Absorption spectra obtained from measurement with (a) Xe/He and (b) Kr/He target. The dotted blue lines illustrate the raw data from the SXR spectrometer. The black lines present data smoothed using the Golay–Savitzky algorithm based on [21] (window = 3 and frame length = 11).
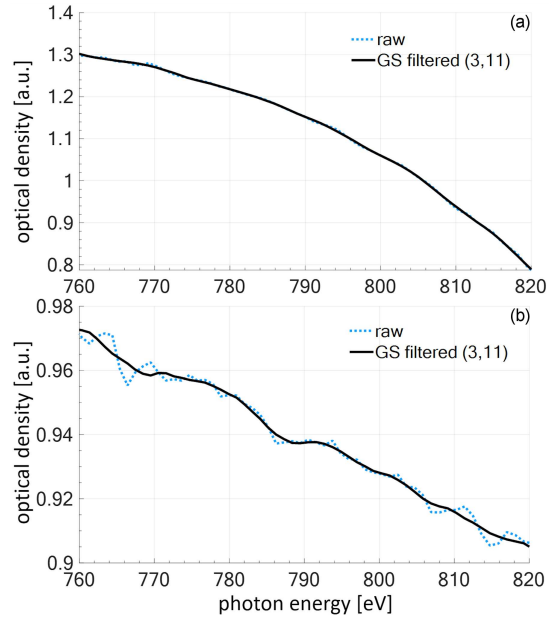
Fig. 4. Absorption spectrum obtained from measurement using the Si_3N_4 membrane without sputtered $B+BaF_2$ layers with (a) Xe/He and (b) Kr/He gas puff target.

absorption spectroscopy performed using the synchrotron radiation to investigate the spectra of $Ba_{1-x}Sr_xCo_{1-y}Fe_yO_{3-\delta}$ (x,y = 0.2–0.8) powders. According to our knowledge, we are the first group that used a compact NEXAFS system to detect barium M-edges in BaF_2.

We investigated whether detected edges are not just artifacts and whether they also occur for measurements done with pure Si_3N_4 membrane (without B and BaF_2 layers). We found no Ba edges, as depicted in Fig. 4a and b for the Xe and Kr illumination source spectrum, respectively.

4. Conclusions

In conclusion, the compact NEXAFS system was used to detect and measure the barium M-edges in the B+BaF_2 optical filter. The results indicate the M5 Ba absorption edge occurring at 780.5 eV, while the M4 edge is found at 796.3 eV for the Xe/He gas puff target and the Ba M5 edge at 780.4 eV for the Kr/He gas puff target. These edges were not visible for pure silicon nitride membranes. We expected to find fluorine K-edge as well, however, due to the nature of fluorine in the BaF_2 compound and the presence of the F–K edge in a spectral region with strong source spectral fluctuation, the signal was insufficient to clearly identify the fluorine K-edge. As for boron, its K-edge was out of the measuring range of the spectrometer.

Acknowledgments

References

[1] J. Stöhr, *NEXAFS spectroscopy*, Vol. 25, Springer, Berlin 2013.

[2] T. Hemraj-Benny, S. Banerjee, S. Sambasivan et al., *Small* **2**, 35 (2006).

[3] P. Guttmann, C. Bittencourt, S. Rehbein, P. Umek, X. Ke, G. Van Tendeloo, C.P. Ewels, G. Schneider, *Nat. Photon.* **6**, 25 (2012).

[4] G. Haehner, *ChemInform* **38** (2007).

[5] D. Li, G.M. Bancroft, M.E. Fleet, *J. Electron Spectrosc. Relat. Phenom.* **79**, 71 (1996).

[6] S.L. Cousin, F. Silva, S. Teichmann, M. Hemmer, B. Buades, J. Biegert, *Opt. Lett.* **39**, 5383 (2014).

[7] A. Jonas, K. Dammer, H. Stiel, B. Kanngiesser, R. Sánchez-de-Armas, I. Mantouvalou, *Anal. Chem.* **92**, 15611 (2020).

[8] W. Błachucki, J. Czapla-Masztafiak, J. Sá, J. Szlachetko, *J. Anal. Atom. Spectrom.* **34**, 1409 (2019).

[9] J. Holburg, M. Müller, K. Mann, P. Wild, K. Eusterhues, J. Thieme, *Anal. Chem.* **94**, 3510 (2022).

[10] D. Hahn, *Opt. Photon.* **9**, 45 (2014).

[11] L. Moliner, G. Konstantinou, J. Maria Benlloch, P. Lecoq, in: *2021 IEEE Nuclear Science Symposium and Medical Imaging Conference (NSS/MIC), Piscataway (NJ)*, 2021, p. 1.

[12] M. Laval, *Nucl. Instrum. Methods Phys. Res.* **206**, 169 (1983).

[13] R.L. Dixon, F.C. Watts, *Phys. Med. Biol.* **17**, 81 (1972).

[14] M.V. Jacob, J.G. Hartnett, J. Mazierska, J. Krupka, M.E. Tobar, *Cryogenics* **46**, 730 (2006).

[15] T. Fok, P. Wachulak, K. Janulewicz, M. Duda, Ł. Węgrzyński, A. Bartnik, R. Jarocki, H. Fiedorowicz, *Acta Phys. Pol. A* **137**, 51 (2020).

[16] H. Fiedorowicz, A. Bartnik, R. Rakowski et al., *J. Phys. IV France* **11**, Pr2-409 (2001).

[17] A. Bartnik, H. Fiedorowicz, R. Jarocki, J. Kostecki, M. Szczurek, P.W. Wachulak, *Nucl. Instrum. Methods Phys. Res. A* **647**, 125 (2011).

[18] P. Wachulak, T. Fok, Ł. Węgrzyński, A. Bartnik, P. Nyga, K. Janulewicz, H. Fiedorowicz, *Opt. Express* **29**, 20514 (2021).

[19] P. Wachulak, M. Duda, A. Bartnik, A. Sarzyński, Ł. Węgrzyński, M. Nowak, A. Jancarek, H. Fiedorowicz, *Opt. Express* **26**, 8260 (2018).

[20] T. Fok, P. Wachulak, Ł. Węgrzyński et al., *Materials* **14**, 7337 (2021).

[21] J. Sedlmair, S.-C. Gleber, C. Peth, K. Mann, J. Niemeyer, J. Thieme, *J. Soils Sediments* **12**, 24 (2012).

[22] B. Ravel, M. Newville, *J. Synchrotron Rad.* **12**, 537 (2005).

[23] T. Hayakawa, M. Arakawa, K. Ando, Y. Kiyomura, T. Kawano, A. Terasaki, *J. Phys. Condens. Matter* **31**, 134003 (2019).

[24] J.Y.P. Ko, Y.-M. Yiu, H. Liang, T.K. Sham, *J. Chem. Phys.* **132**, 234701 (2010).

[25] A.S. Harvey, Z. Yang, A. Infortuna, D. Beckel, J.A. Purton, L.J. Gauckler, *J. Phys. Condens. Matter* **21**, 015801 (2008).